Relation of Enzyme Activity to Local/Global Stability of Murine Adenosine Deaminase: 19F NMR Studies

ARTICLE *in* JOURNAL OF MOLECULAR BIOLOGY · FEBRUARY 2005

Impact Factor: 4.33 · DOI: 10.1016/j.jmb.2004.10.057 · Source: PubMed

2 AUTHORS, INCLUDING:

Qin Shu
Washington University in St. Louis
13 PUBLICATIONS **271** CITATIONS

doi:10.1016/j.jmb.2004.10.057 J. Mol. Biol. (2005) 345, 599–610

JMB

Available online at www.sciencedirect.com

SCIENCE DIRECT®

ELSEVIER

Relation of Enzyme Activity to Local/Global Stability of Murine Adenosine Deaminase: ^{19}F NMR Studies

Qin Shu and Carl Frieden*

Department of Biochemistry and Molecular Biophysics Washington University School of Medicine, 660 South Euclid Avenue, Campus Box 8231 St Louis, MO 63110, USA

Adenosine deaminase (ADA, EC 3.5.4.4) is a ubiquitous $(\beta/\alpha)_8$-barrel enzyme crucial for purine metabolism and normal immune competence. In this study, it was observed that loss of enzyme activity of murine ADA (mADA) precedes the global secondary and tertiary structure transition when the protein is exposed to denaturant. The structural mechanism for this phenomenon was probed using site-specific ^{19}F NMR spectroscopy in combination with [6-^{19}F]tryptophan labeling and inhibitor binding. There are four tryptophan residues in mADA and all are located more than 12 Å from the catalytic site. The ^{19}F NMR spectra of [6-^{19}F]Trp-labelled mADA show that the urea-induced chemical shift change of ^{19}F resonance of W161, one of the four tryptophan ^{19}F nuclei, correlates with the loss of enzyme activity. The urea-induced chemical shift change of another ^{19}F resonance of W117 correlates with the change of the apparent rate constant for the binding of transition-state analogue inhibitor deoxycoformycin to the enzyme. On the other hand, the chemical environment of the local region around W264 does not change significantly, as a consequence of perturbation by low concentrations of urea or substrate analog. The results indicate that different regions of mADA have different local stability, which controls the activity and stability of the enzyme. The results provide new insights into the relationship between the function of a protein and its conformational flexibility as well as its global stability. This study illustrates the advantage of ^{19}F NMR spectroscopy in probing site-related conformational change information in ligand binding, enzymatic activity and protein folding.

Keywords: (β/α)8-barrel; protein unfolding; chemical shift; substrate binding; local stability

*Corresponding author

Introduction

Many proteins are known to undergo conformational changes on interacting with substrates, ligands or other macromolecules that regulate their biological function, even though the proteins maintain their global stable and folded structures. Both conformational flexibility and global stability are required for a protein to be functional in the cellular environment. Understanding the relationship between the conformational flexibility and the function of a protein, such as enzyme catalysis, remains a fundamental issue, as is the relationship of the local conformational flexibility to the overall stability.

The $(\beta/\alpha)_8$ or triose phosphate isomerase (TIM) barrel, consisting of eight parallel central β-strands and eight peripheral α-helices, is one of the most commonly observed protein folds.[1,2] Almost all $(\beta/\alpha)_8$-barrel proteins are enzymes, even though they have very low levels of sequence identity and diverse catalytic functions. Because of the remarkable versatility and their relative abundance, the $(\beta/\alpha)_8$-barrel proteins have been investigated extensively in terms of structure, function, folding and evolution.[3–9] The folding and stability properties of the $(\beta/\alpha)_8$-barrel have been proposed to be a reason for the frequent occurrence of this super structure fold.[10]

Adenosine deaminase (ADA, EC 3.5.4.4) is a zinc-containing $(\beta/\alpha)_8$-barrel enzyme (Figure 1)[11]

Abbreviations used: ADA, adenosine deaminase; mADA, murine adenosine deaminase; GdnHCl, guanidine hydrochloride; DCF, deoxycoformycin; PR, purine riboside; HDPR, 6-hydroxyl-1,6-dihydropurine ribonucleoside.

E-mail address of the corresponding author: frieden@biochem.wustl.edu

that catalyzes the irreversible deamination of adenosine or 2′-deoxyadenosine to inosine or 2′-deoxyinosine and ammonia. It is a key enzyme in purine metabolism and is required for normal immune competence. ADA deficiency accounts for about 15% of all cases of severe combined immunodeficiency (SCID) syndrome, and a third of those with autosomal recessive inheritance.[12,13] In this study, the unfolding/stability of murine ADA (mADA) and its relationship to the enzyme activity were investigated using a multifaceted approach combining urea-induced denaturation and enzyme activity with optical and ^{19}F NMR spectroscopy.

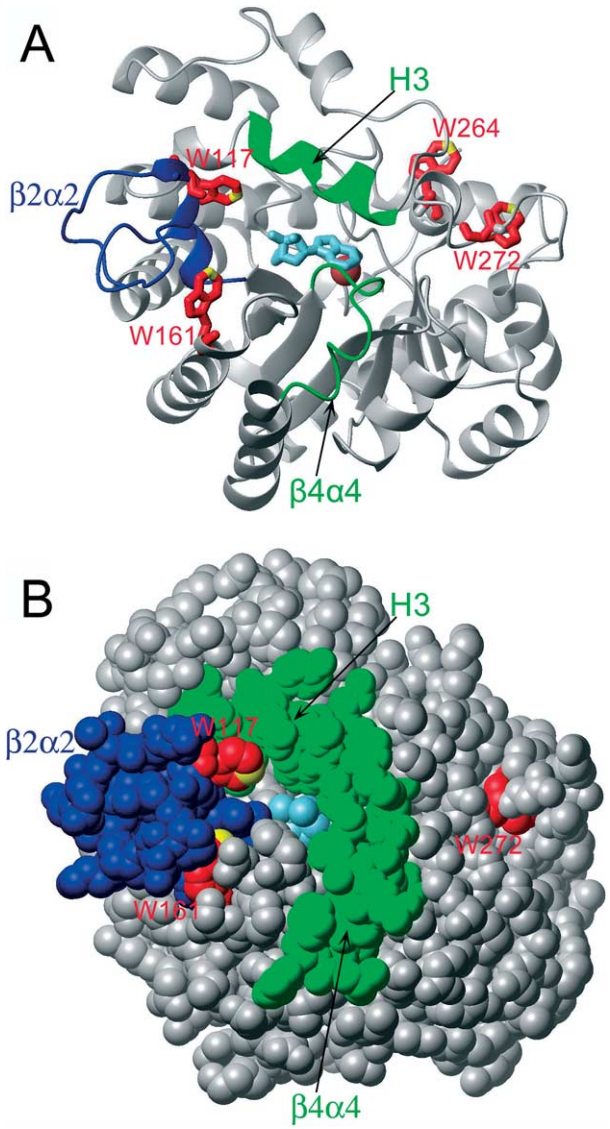

Figure 1. MOLMOL[42] representation of murine adenosine deaminase (mADA), a zinc-containing $(\beta/\alpha)_8$-barrel enzyme (viewed from the top of the active pocket). A, Ribbon representation. B, Space-filling representation. The metal cofactor zinc ion (shown in brown) and the substrate analogue (shown in light blue) are located in the center of the active pocket. The four tryptophan residues (W117, W161, W264 and W272) are shown in red, except that the fluorinated C-6 atoms on each indole ring are shown in yellow. Residues 58–67 located in the helix H3 and residues 183–188 located in loopβ4α4 (both shown in green) form partial lids of the active pocket, shielding the substrate analogue.[11] The loop β2α2 (shown in blue) is where W117 is located (see Discussion).

We show that mADA loses enzyme activity at low concentrations of the denaturants urea and guanidine hydrochloride (GdnHCl), even though, as shown by circular dichroism (CD) and fluorescence spectroscopy, the protein retains its native secondary and tertiary structure. In our previous study of [6-^{19}F]tryptophan-labelled mADA,[14] non-uniform unfolding was revealed by using ^{19}F NMR. Although the denaturation curve appeared to follow a simple two-state behavior, as monitored by CD and fluorescence, the chemical shifts of the ^{19}F resonances of the four [6-^{19}F]Trp residues exhibited different urea-dependent changes, indicating that different local regions in mADA were perturbed differently by urea, and that these changes occurred prior to the global secondary and tertiary structure transition. We now find that the urea-induced chemical shift change of the ^{19}F resonance of W161, one of the four tryptophan residues, correlates with loss of enzyme activity, and that of another, W117, correlates with a change in the apparent rate constant of deoxycoformycin (DCF) (a transition-state substrate analog) binding to the enzyme. These observations led us to apply the site-specific ^{19}F NMR technique to detect the conformational change information of the protein at low concentrations of denaturant.

Results

Enzyme activity of ADA as a function of urea concentration

The decrease in enzymatic activity as a function of concentration of denaturant precedes the global secondary or tertiary structure change, as measured by CD or fluorescence spectroscopy, when mADA is unfolded by urea (Figure 2A) or by GdnHCl (Figure 2B; Table 1).

The loss of enzyme activity induced by low concentrations of urea occurs rapidly, being too fast to be measured even by stopped-flow methods, as illustrated in Figure 3B, where k_{cat} of mADA as a function of urea concentration shows no obvious difference for the sample equilibrated in urea for two hours or for less than 5 ms. On the other hand, denaturation in terms of secondary and tertiary structure change is time-dependent, requiring up to 22 hours before reaching the final curves shown in Figure 2.

The urea-induced zinc dissociation from mADA is very slow,† so that the urea-induced loss of

† Dissociation of zinc from mADA at different denaturant concentrations can be monitored by the fluorescence increase of Fura-2 (λ_{Ex} = 330 and λ_{Em} = 505 nm). In the presence of either 2 M Gdn or 8 M urea, zinc dissociation from the protein is of the order of hours.

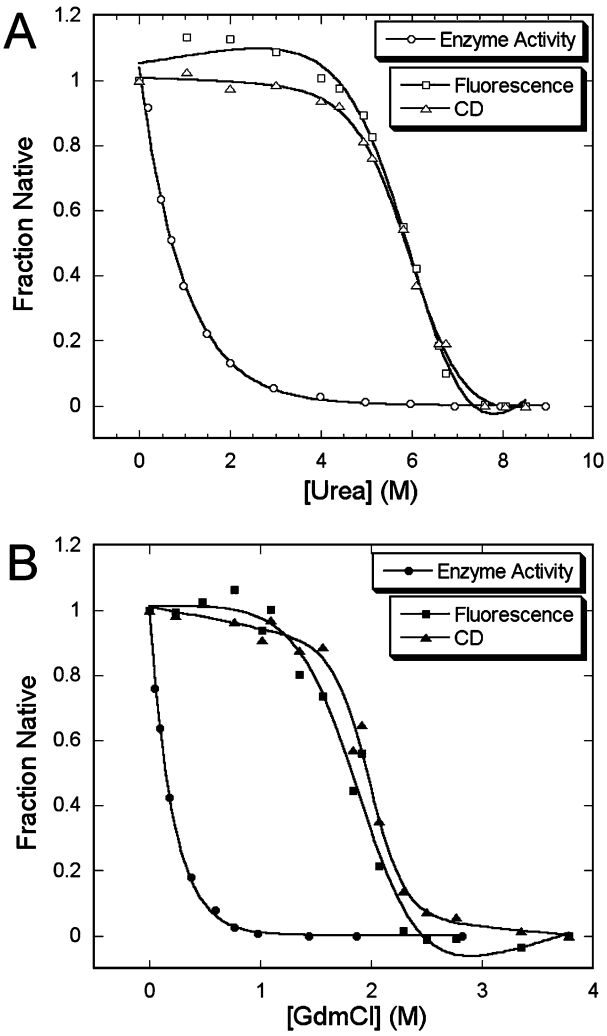

Figure 2. Comparison of mADA unfolding as monitored by enzyme activity (fit to the single-exponential function), ellipticity at 222 nm (fit to the two-state model[41]), and fluorescence intensity using λ_{em} 330 nm and λ_{ex} 290 nm (fit to the two-state model[41]). A, Unfolding induced by urea. B, Unfolding induced by GdnHCl. All experiments were performed in 20 mM Tris–HCl (pH 7.4), 2 mM DTT, at 20 °C. Samples for CD and fluorescence experiments were equilibrated in urea for 22 hours before measurement. Samples for enzyme assay were equilibrated in urea for 22 hours before measurement, although the enzyme activity change is independent of the pre-equilibrium time in denaturant (see Results). The thermodynamic parameters are shown in Table 1.

enzyme activity is not due to the loss of zinc, a cofactor located at the active site and required for catalytic activity (Figure 1).[11,15]

Kinetic studies

In previous studies, we have shown that the kinetic mechanism of ADA can be represented by a simple scheme:[16]

$$E + A \rightleftharpoons EA \rightleftharpoons EP \rightarrow E + P$$

Kinetic parameters can be obtained by analysis of the progress curve using the program KINSIM,[17] as described by Kurz *et al*.[16] The kinetic parameters of native mADA for adenosine are $K_m \sim 19\ \mu M$ and $k_{cat} \sim 250\ s^{-1}$ at pH 7.4 and 20 °C. The kinetic parameters of mADA at different concentrations of urea were determined and are shown in Figure 3A and B. The data show that the change in enzymatic activity as a function of urea concentration is a consequence of a change in k_{cat} (Figure 3B) rather than K_m (Figure 3A).

The transition-state substrate analog inhibitor deoxycoformycin (DCF) is known to bind tightly to native mADA.[18] We find that it can bind to the enzyme equilibrated in concentrations of urea up to 6 M for 22 hours but not to the completely denatured mADA (8 M urea, equilibrated for 22 hours) as measured by quenching of the intrinsic fluorescence of the protein (data not shown). We had shown that the mechanism for DCF inhibition is an initial weak binding followed by a conformational change leading to tight binding, the process being characterized as an apparent slow binding step.[19,20] This process can be followed by a time-dependent decrease in protein intrinsic fluorescence. Figure 4A shows that the apparent rate constant of DCF binding to mADA decreases as a function of urea concentration. Figure 4B shows the correlation between the urea-induced change of the apparent rate constant for DCF binding to mADA and the chemical shift behavior of the ^{19}F resonance of W117 (discussed below).

In addition, DCF inhibition of ADA activity is a time-dependent process that is characterized by an apparent slow on rate constant.[19] We have measured the rate of inhibition as a function of urea and found that these values correlate with the change in the rate of DCF binding (data not shown).

Since low concentrations of urea do not affect the Michaelis constant, the loss of enzyme activity is not due to a specific competition of urea with the substrate or substrate analog at the active site.

Structural properties of partly or completely inactive folding intermediates

The four tryptophan residues (W117, W161, W264, and W272) of mADA are located in different elements of secondary and tertiary structure of the $(\beta/\alpha)_8$-barrel and more than 12 Å from the catalytic site that is centered at C-6 of the purine ring of the substrate and the cofactor zinc (Figure 1; Table 2). In our previous study of the denaturation,[14] a two-state model with a midpoint at about 6 M urea fits the data as monitored by CD or fluorescence spectroscopy. The ^{19}F NMR studies reveal, however, that the chemical shifts of the four folded ^{19}F resonances in [6-^{19}F]Trp-labelled mADA exhibited different urea-dependent changes well below 6 M urea. Thus, the protein unfolds non-uniformly, and

Table 1. Thermodynamic parameters of mADA

Experiment	Denaturant	ΔG^0 (kcal mol^{-1})	m (kcal mol^{-1} M^{-1})	[Denaturant]$_{1/2}$ (M)
Fluorescence intensity[a]	Urea	4.89	0.79	6.19
Far-UV CD $\theta_{222\ nm}$[a]	Urea	5.78	0.96	6.02
Enzyme assay[b]	Urea	N/A	N/A	0.68
Fluorescence intensity[a]	GdnHCl	3.98	2.08	1.91
Far-UV CD $\theta_{222\ nm}$[a]	GdnHCl	7.39	3.73	1.98
Enzyme assay[b]	GdnHCl	N/A	N/A	0.15

All experiments were performed in 20 mM Tris–HCl (pH 7.4), 2 mM DTT, at 20 °C.

[a] The fluorescence and CD data were derived from Figure 2A (urea) and B (GdnHCl). Values for ΔG^0, the cooperativity index (m), and the midpoint ([Denaturant]$_{1/2}$) were determined by fitting the data to a two-state model.[41]

[b] The enzyme assay data, from Figure 2A (urea) and B (GdnHCl), could not be fit to the simple ligand-binding function, suggesting a complicated mechanism for the effect of urea on the enzyme. The midpoint was determined by fitting data to a single-exponential function.

different local regions of mADA are affected by urea differently.

Since a correlation between the chemical shift behavior of ^{19}F resonance for W161 and the loss of the enzyme activity at low concentrations of urea was observed, the equilibrium chemical shift behavior of mADA was reinvestigated using lower concentrations of urea (below 1 M). The results, combined with our previous data[14] are shown in Figure 5A and B. Consistent with our previous data at higher concentrations of urea,[14] different Trp ^{19}F resonances show different urea-dependent chemical shift changes when the concentration of urea is less than 1 M. The results can be divided into two sets according to their correlation with the enzyme activity change. One set contains W264 and W272, where the chemical shift behavior shows no correlation with the change in enzyme activity. A small linear chemical shift change of W264 (the most solvent-exposed tryptophan residue) upon addition of urea is due to a solvent effect rather than a conformational change (unpublished data). W272 has a large linear chemical shift change that we presume to be a change in the local chemical environment. The other set contains W117 and W161, where the urea-induced chemical shift change is related to the enzyme activity change. The chemical shift change of W161 exactly mirrors the enzyme activity change of mADA, as illustrated in Figure 5C. The chemical shift change of W117 is complex, containing both downfield and upfield shifts. The data were best fit to a two-parameter function, a single-exponential plus a linear phase, which reflects a complex chemical environment change at this region. The single-exponential behavior of W117 correlates with the urea-induced decrease of the apparent rate constant for DCF binding to mADA (Figure 4B). A complex behavior is observed also in chemical shift changes of W117 induced by different inhibitors (shown below), which further confirms a relationship between the local chemical environment of W117 and the enzyme function.

Thus, in the presence of low concentrations of urea, some regions of the protein, such as those around W264, are resistant to perturbation by urea and preserve their native local structure, some regions, such as those around W272, may have conformational changes that are unrelated to the urea-induced enzyme activity change, while other regions, such as W117 and W161, have local environmental changes related to the urea-induced enzyme activity change. Since low concentrations of urea do not disrupt the global native secondary and tertiary structure, it might be expected that most local regions of the protein should be highly resistant to urea and behave like that around W264. The change in activity of mADA at low concentrations of urea is due to subtle urea-dependent local conformational changes at certain regions, such as those around W117 and W161, even though they are more than 12 Å from the catalytic site.

Conformational changes induced by substrate analogue

It is widely believed that substrate binding plays a key role in inducing and optimizing catalytic conformational changes in enzymes. The ^{19}F NMR spectra of mADA bound with the transition-state substrate analogue DCF and the ground-state substrate analogue purine riboside (PR) were collected to provide information about the substrate analogue-induced local chemical environment change of the Trp ^{19}F resonances.

Compared to the free native enzyme, the ^{19}F NMR spectrum of mADA containing DCF (Figure 6, +DCF) shows that the chemical shifts of all resonances except that of W264 have moved downfield. The spectrum of mADA containing PR (Figure 6, +PR) shows that the resonances of W161 and W272 move downfield. There is no obvious change for W264, while the resonance of W117 shifts upfield.

Different chemical shift behavior of the four Trp ^{19}F nuclei induced by inhibitor binding are observed in the ^{19}F NMR spectra, demonstrating that different local regions undergo different conformational changes upon substrate binding. Thus, the chemical shift behavior of these Trp ^{19}F nuclei of mADA can be used to probe the subtle structural information related to the enzyme functional process.

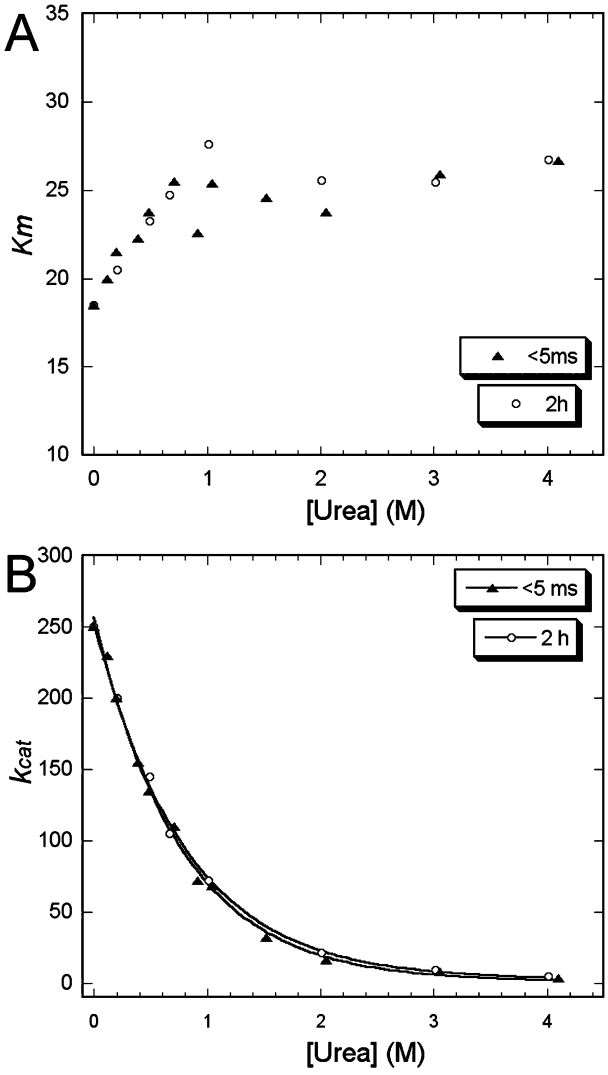

Figure 3. Kinetic parameters of mADA as a function of urea concentration. A, K_m, the Michaelis constant; B, k_{cat}. The enzyme was pre-equilibrated in urea for two hours (open circles) prior to stopped-flow measurement or added to a substrate/urea mixture to initiate the reaction by stopped-flow (dead-time <5 ms) (filled triangles). The K_m and k_{cat} for native mADA from three separate experiments are 19(±5) μM and 250(±20) s^{-1}, respectively. The k_{cat} of mADA as a function of urea concentration was fit as a single-exponential function with a urea midpoint about 0.56 M (two hours) or 0.53 M (< 5 ms). All experiments were performed in 20 mM Tris–HCl (pH 7.4), 2 mM DTT, at 20 °C.

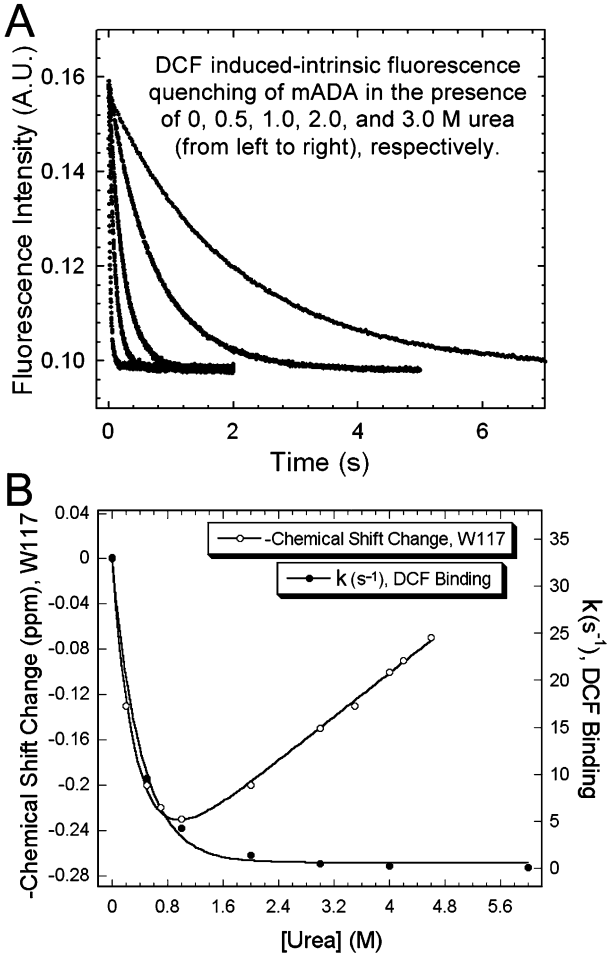

Figure 4. A, The time-course of DCF-induced intrinsic fluorescence quenching of native mADA (0 M urea) and mADA denatured by 0.5 M, 1.0 M, 2.0 M, and 3.0 M urea, respectively. The concentrations of mADA and DCF were 0.25 μM and 5 μM, respectively, using as the buffer 20 mM Tris–HCl (pH 7.4), 2 mM DTT. All measurements were performed at 20 °C. B, Comparison of the apparent rate constant of DCF binding to mADA (k, s^{-1}) and the chemical shift change of ^{19}F resonance for W117 as a function of urea. The apparent rate constants of DCF binding to mADA (k, s^{-1}) at different concentrations of urea were determined by using computer simulation of the full time-course. The change of k (s^{-1}, DCF binding) as a function of urea concentration was fit to a single-exponential function with a midpoint about 0.28 M urea. The chemical shift changes of ^{19}F resonance for W117 upon urea are from Figure 5A and B, fit to a single-exponential plus a linear phase.

Comparison of urea and substrate analogue-induced chemical shift changes

As indicated above, the chemical shift change of W117 shows a complex behavior, the resonance shifting downfield in the presence of DCF, upfield in the presence of PR, and both downfield and upfield in the presence of urea. The complex behavior of the chemical shift of W117 induced by different inhibitors is consistent with the complex behavior of this resonance induced by urea. There is a direct correlation between the urea-induced apparent rate constant change of DCF-binding to mADA and the single-exponential part of the urea-induced chemical shift change of W117. Although W117 is more than 14 Å from the catalytic center, the closest distance between the side-chain of W117 and the sugar group of the substrate analogue is about 6 Å (Figure 1; Table 2). These data support the idea that the local region around W117, located in the

Table 2. Structural environment of Trp residues of mADA

Residue	Secondary structure	Distance of C^{α} to zinc (Å)	Closest distance of side-chain to zinc (Å)	Closest distance of C^{α} to substrate (Å)	Closest distance of side-chain to substrate (Å)
W117	Loop β2α2	20.1	14.5	11.3	6.2
W161	α3	18.2	15.6	12.8	8.9
W264	Loop β7α7	12.0	12.3	11.0	12.3
W272	Loop β7α7	14.3	14.0	12.6	12.4

The distances were from the crystal structure of complex of mADA (PDB ID 2ADA,[11] 1A4M and 1A4L[22]). Loop β2α2, where W117 is located, connects the central β2 strand and the peripheral α2 helix. Loop β7α7, where W264 and W272 are located, connects the β7 strand and the α7 helix. W161 is located in the α3 helix.

loop β2α2 (Figure 1, shown in blue), is involved in a conformational change during substrate and substrate analogue binding.

The chemical shift of W161 induced by urea or inhibitor (DCF or PR) moves downfield. Although the closest distance of W161 to the catalytic center (zinc) and the substrate analogue is about 15.6 Å and 8.9 Å, respectively, the urea-induced chemical shift behavior of W161 correlates with the loss of enzymatic activity. As discussed below, the chemical shift change of W161 might primarily reflect the conformation change of loop β2α2.

The chemical shift of W264 is insensitive to both inhibitor binding and concentration of denaturant, even though W264 is more exposed to solvent than other Trp residues (solvent accessibility ~60%). The chemical shift behavior of W264 suggests a high local stability of this region. Although located in the same loop as W272, β7α7, W264 is located within a short helix (263–268). This local ordered secondary structure might improve the local stability of W264. As discussed above, because the global native secondary and tertiary structure are preserved at low concentrations of urea, most local regions of mADA should have high local stabilities and behave like W264. The high level of local stability of structural elements with highly ordered secondary structure should contribute to the high level of stability of the global structure of the enzyme.

For W272, the DCF-induced or PR-induced downfield shift is different from the urea-induced linear upfield shift change, suggesting that the chemical environmental changes caused by urea or inhibitor at the local region around W272 are different.

Peak broadening of the resonances of W117 and W161, but not those of W264 and W272, was observed in the presence of inhibitors (Figure 6). The linewidth of the resonances of W117 and W161 increase from about 77 Hz and 65 Hz to about 99 Hz and 81 Hz, respectively, in the DCF-bound form and to about 120 Hz and 99 Hz, respectively, in the PR-bound form. In contrast, the linewidth of the resonances of W264 and W272 remain about 66 Hz upon different inhibitor binding. Linewidth analysis had shown that ^{19}F resonances of W117 and W161 are peak broadened with increasing concentration of urea but those of W264 and W272 are not.[14] Similar peak broadening of the resonances of W117 and W161 induced by inhibitor or urea suggests that inhibitor binding or urea perturbation affect the dynamics or chemical environment of the local region around W117 and W161.

In sum, different Trp ^{19}F resonance of mADA shows different chemical shift behavior upon urea-induced perturbation or substrate analogue binding, suggesting that different structural elements have different local stability and are involved in the catalysis differently. The subtle local structural changes at certain regions lead to the loss of enzyme activity that precedes the global structure transition during unfolding.

Discussion

Here, we have used different techniques to investigate the enzymatic activity and the local/global structural changes of mADA upon denaturant or inhibitor-induced perturbation. The results provide new insights into the conformational flexibility, the folding/stability and their relationship with the activity of this $(\beta/\alpha)_8$-barrel enzyme.

Structural significance of ^{19}F chemical shift change

The structural significance of a chemical shift change is key for this investigation. Although the chemical shifts of ^{19}F are known to be extremely sensitive to local conformational environment, including van der Waals packing interactions and local electrostatic fields,[21] it is not currently possible to convert the magnitude or the sign of a chemical shift to any direct distance or spatial change. In order to avoid an over-interpretation of our current ^{19}F NMR data, the structural significance of the chemical shift change of the Trp ^{19}F resonances were analyzed on the basis of the available high-resolution crystal structures of ADA, recognizing that a crystal structure may reflect averages of many dynamic structures.

The chemical shift changes of W117 in DCF-bound mADA are significantly different from those in PR-bound mADA. However, a comparison of the region around W117 (within 5 Å) in crystal structures of mADA bound with DCF[22] or PR[11,22] shows no obvious difference in terms of the side-chain or

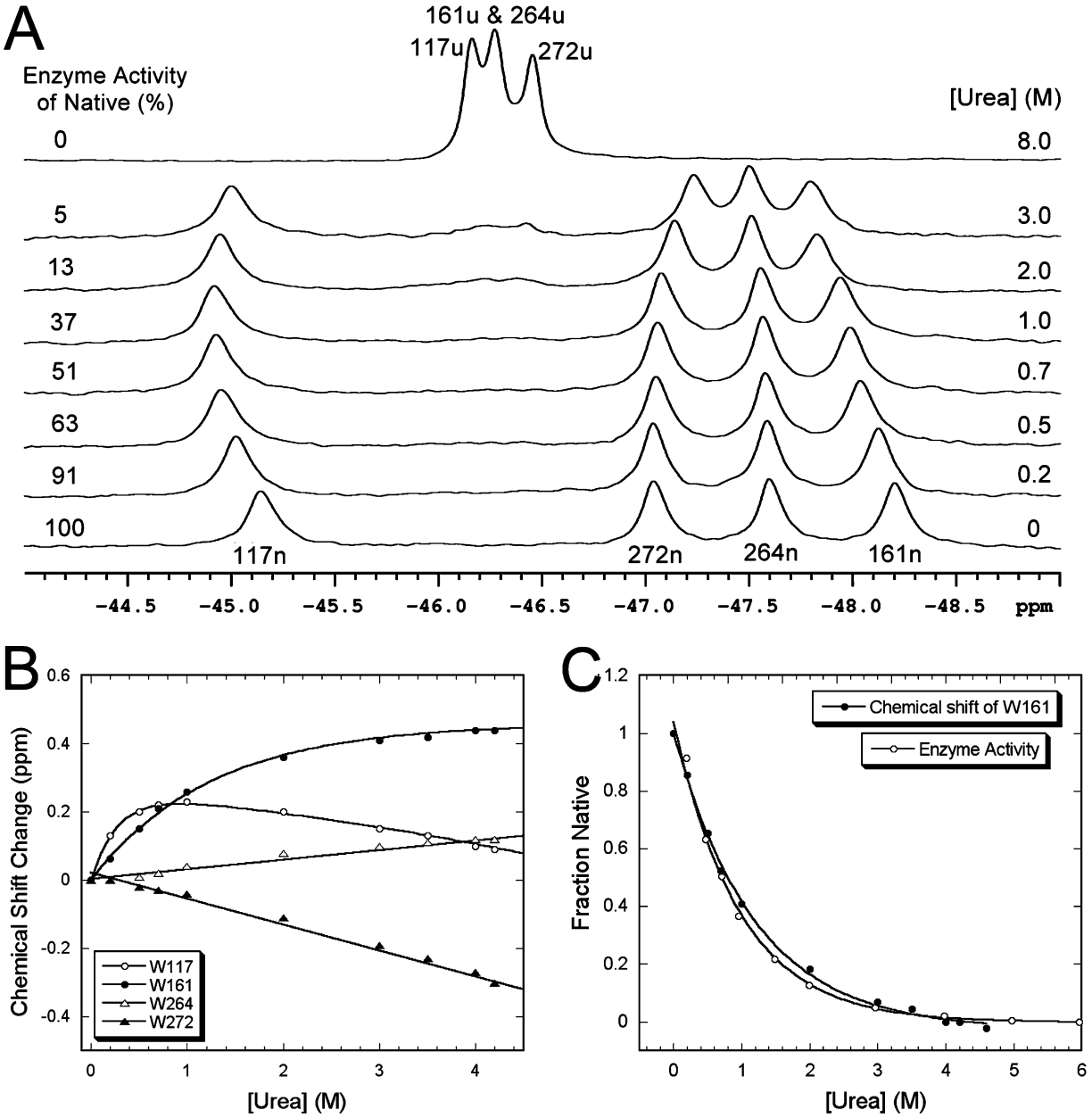

Figure 5. Equilibrium unfolding of mADA as monitored by ^{19}F NMR. A, ^{19}F NMR spectra of mADA at the indicated concentration of urea. [6-^{19}F]Trp-labelled mADA (85 μM) was equilibrated at the indicated concentration of urea in 20 mM Tris–HCl (pH 7.4), 2 mM DTT, at 20 °C for 22 hours before collection of the NMR spectra. B, Chemical shift change of Trp ^{19}F resonances as a function of the concentration of urea. Data are derived from A and from Wang & Quiocho.[22] The chemical shift change of ^{19}F resonance for W117 was fit to a single-exponential (k_1=2.92) plus a linear function (k_2=−0.049); that for W161 was fit to a single-exponential function with a urea midpoint about 0.83 M; 264 and 272 were fit to linear curves with a slope of 0.028 and −0.076, respectively. C, Comparison of the chemical shift change of the ^{19}F resonance for W161 and the enzyme activity change upon urea unfolding. The chemical shift change of ^{19}F for resonance W161 was normalized to the fraction native using the equation: $F = (\delta - \delta_{4.6})/(\delta_n - \delta_{4.6})$, where δ represents chemical shift for the native state (δ_n) or the intermediate state ($\delta_{4.6}$) at 4.6 M urea. The enzyme activity change upon urea unfolding was from Figure 2A. Both curves were fit to a single-exponential function; the urea midpoints are 0.83 M for the chemical shift change of ^{19}F resonance for W161 and 0.68 M for the enzyme activity change, respectively.

backbone. This raises questions about the structural significance of the chemical shift change observed for these Trp ^{19}F resonances, i.e. whether the conformational changes of mADA induced by low concentrations of urea or inhibitor are really very small (within 1 Å) or whether the crystal structure does not reflect structural fluctuations.

In contrast to the crystal structure data, we believe that the chemical shift changes of these Trp ^{19}F resonances in mADA induced by low concentrations of urea or inhibitor do indicate significant changes in local chemical environment as well as local structure. First, conformational changes induced by ligand binding were proposed

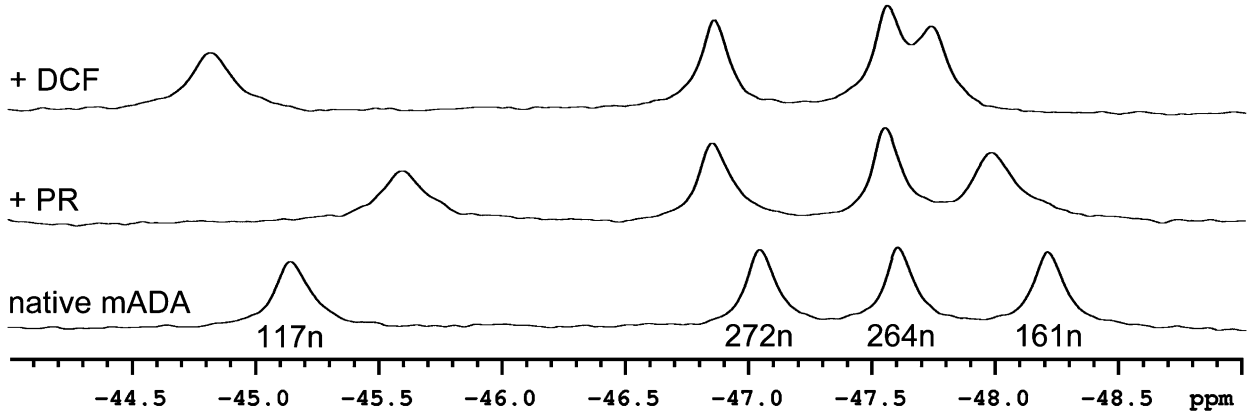

Figure 6. Comparison of ^{19}F NMR spectra of free native mADA and different inhibitor-bound mADA. The concentration of mADA was 100 μM and the concentration of DCF or PR was 200 μM. All samples were equilibrated in 20 mM Tris–HCl (pH 7.4), 2 mM DTT at 20 °C for 22 hours before collecting the NMR spectra.

in enzyme mechanism studies[19,20] and in the crystallographic studies[11]. In the crystal structure of the complex of mADA with 6-hydroxyl-1,6-dihydropurine ribonucleoside (HDPR), the HDPR moiety is almost completely inaccessible to solvent. Two loops (residues 58–67 in helix H3 and residues 183–188 in loop β4α4) form partial lids over the active-site pocket (Figure 1A and B, shown in green). Thus, there must be a transient dynamic conformational change that allows the substrate to enter the active-site pocket.

Secondly, the loop β2α2 (residues 103–125) (Figure 1A and B, shown in blue), where W117 is located, should be involved in the conformational change during substrate binding, as suggested by the urea-dependent correlation between the ^{19}F NMR signal change and the change of the rate constant for DCF binding to mADA. In the crystal structure, the loop β2α2 is located near the side of the sugar group of the substrate analogue but far from the catalytic center of the C-6 of the purine and the cofactor zinc ion (Figure 1A; Table 2), which provides a structural rationale for its involvement in substrate binding.

Moreover, the only reported *cis*-prolyl peptide bond (P114) among the 18 proline residues in mADA is located in the loop β2α2 (PDB ID 1A4M[22]). The crystal structure data concerning the configuration of the prolyl imide bond at position 114, however, are not consistent. Both *cis* and *trans* configurations have been reported in complex structures of mADA:HDPR (PDB ID 2ADA[11], 1A4M[22]). The only reported structure of an mADA:DCF complex is a *trans* configuration for the prolyl-peptide bond of P114 (PDB ID 1A4L[22]). It is not clear whether this is caused by some structural disorder at this region leading to a crystallographic artifact or whether it is a case of native-state peptide prolyl *cis*/*trans* isomerization for substrate binding and function regulation. Summarizing, we believe that the loop β2α2, where W117 is located, is involved in the conformational change during substrate binding; W161 may be involved in the conformational change of the loop β2α2 through a hydrogen bond, depending on the *cis*/*trans* configuration of P114.

We note that the loop β2α2, especially the positions near the sugar group of the substrate analogue, is a region of high frequency of ADA mutations leading to ADA deficiency-related immune dysfunction. For example, the mutations of P104L, L106V[23] and L107P[13,24] (all close to W117) are clinically significant. Several SCID or partial ADA deficiency-related mutations such as G74V, G74D, G74C, P126Q and V129M[13,24,25] have direct structural relationship with this loop. The mechanism of ADA deficiency in these naturally occurring mutants is not very clear, even with the available crystal structure. These mutations may affect the local structure and flexibility/stability of the loop β2α2 and lead to a change in ADA activity.

Structural mechanism of denaturant-induced ADA inactivation

Activity measurements are not used widely in folding studies, since there is the possibility of inhibition by the denaturant itself. However, there are a large number of enzymes that have been shown to lose activity in response to chemical denaturants or physical factors (such as temperature or pressure) prior to the global structure denaturation.[26–29] Tsou and co-workers have observed that the conformation of the active site is indeed perturbed under mild denaturation conditions, as examined by fluorescent[30,31] or ESR[32] probes introduced into an enzyme active site or using partial proteolysis.[33] These observations give rise to the suggestion that enzyme active sites are more flexible and more sensitive to denaturation than the molecule as a whole, and that the conformational flexibility of the active site is essential for the full expression of enzyme activity.[26–33]

In this study, the addition of urea or GdnHCl results in loss of mADA enzyme activity preceding

the global secondary and tertiary structure transition. Our investigation, especially by ^{19}F NMR, provides new information on the structural mechanism of this phenomenon. The results show that different regions of mADA have different local stability that control the function and global stability of the enzyme. All Trp residues of mADA are more than 12 Å from the catalytic site, which is too large for direct interaction to affect the catalytic reaction. The effect of low concentrations of denaturant on the catalytic site is not clear from our current data. Our results suggest that the correlated change of local structure around W117 and W161 and the enzyme activity in the presence of denaturant should be related to substrate binding through a propagated structural effect, and a specific local environment, even in regions distant from the catalytic site, is required for catalysis.

We concluded previously that the formation of a tetrahedral intermediate is the most difficult chemical step in the enzymatic mechanism.[34] If the mechanism is not changed in the presence of denaturant, then subtle conformational changes in the loop β2α2 around W117 and W161, even though they are distant from the catalytic reaction center, somehow affect the formation of the tetrahedral intermediate, presumably through conformational change propagated through the structure. The naturally occurring disease-related ADA mutants around the loop β2α2 provide an indirect support of our conclusion.

Separate roles of the structural elements for activity and stability

The function of an enzyme depends on the conformational flexibility and the stability of its native three-dimensional structure *in vivo*. An investigation of the structural mechanism for activity and stability in enzymes could help our understanding of the mechanism of enzyme catalysis, enzyme engineering and enzyme-targeted drug design.

In all $(\beta/\alpha)_8$ enzymes, despite the diversification in catalytic residues and substrate specificities, the active sites are funnel-shaped pockets formed by the C-terminal ends of the eight β strands and the βα loops that link β strands with the subsequent α helices. In contrast, the loops, locating at the back side of the barrel and linking the α-helices with the subsequent β-strands, are believed to be involved in protein stability.[9,35] The spatial separation of regions important for activity and for stability is thought to be important for enzymes, which allows conformational changes during the ligand/substrate binding, catalysis or the allostery regulation process and maintains the global stable native structure of a protein.[9,35]

The difference between the enzyme activity change and the global structure change observed in mADA confirms separate roles of structural elements for function and for stability in this $(\beta/\alpha)_8$-barrel enzyme. The site-specific ^{19}F NMR studies of mADA suggest that the separate roles for function and for stability in the enzyme is due to differences in the local stability of different structural elements of the protein. On the other hand, we are not able to assess the role of the loops for stability from the current data, since all Trp residues of mADA are located in the βα loops for activity. Introducing ^{19}F probes into specific sites of the protein can be used to address the role of the loops for stability in $(\beta/\alpha)_8$ enzymes. Due to the high sensitivity of ^{19}F nuclear spin, the large chemical shift resolution, the ability to incorporate the label at specific sites and minimal perturbation of the protein structure, ^{19}F NMR should be able to be applied widely in probing site-related conformational change information in ligand binding, enzymatic activity and folding studies of proteins as illustrated in this study.

Murine ADA is not the first $(\beta/\alpha)_8$-barrel enzyme in which the phenomenon of inactivation preceding the global structure transition has been observed. In folding studies of indole-3-glycerol-phosphate synthase (IGPS), the enzyme activity is lost, in a cooperative way, at a lower concentration of urea than the denaturation as measured by fluorescence.[36] At low concentrations of denaturant, IGPS loses its activity to produce an intermediate species with spectroscopic and hydrodynamic properties very similar to those of the native form.[36] Multiple intermediates and/or folding units have been observed in other $(\beta/\alpha)_8$-barrel proteins as detected by different techniques,[7,8,36–40] but the folding mechanism of $(\beta/\alpha)_8$-barrel proteins is still ambiguous because of the complexity of the folding behavior of these proteins. The properties of mADA upon denaturant perturbation, especially the local stability and the relation to the function, provide new clues to reveal the folding/stability mechanism of other $(\beta/\alpha)_8$-barrel proteins.

In conclusion, the investigation of mADA by ^{19}F NMR spectroscopy in combination with [6-^{19}F]Trp labeling and substrate analogue binding provides insights into the structural mechanism of loss of enzyme activity at low concentrations of denaturant. Current ^{19}F NMR studies of mADA indicate that different local regions of the protein have different local stabilities and are involved in the catalysis differently. Most of the local regions with the highly ordered secondary structure, such as that around W264, are as stable as the global structure of the protein; and some local regions such as those at the loop β2α2 around W117 and W161 are more sensitive to environmental change than the protein as a whole, which fills the requirement for the ligand/substrate binding and catalysis process. As a consequence of perturbation in low concentrations of urea, the molecules of mADA retain the global native secondary and tertiary structure but are partly or completely inactive due to subtle conformational changes at certain local regions (such as the loop β2α2 around W117 and W161). The difference between the loss of enzyme activity and the change of the global structure during mADA unfolding relies on the different local

stability of those different structural elements responsible for enzyme activity or for overall folding and stability of the protein molecule.

Materials and Methods

Materials

Adenosine, purine riboside (PR) and 6-fluoro-D,L-tryptophan were purchased from Sigma. Deoxycoformycin (DCF) was from the Developmental Therapeutic Program, National Cancer Institute. Ultrapure urea and GdnHCl were products of United States Biochemical. The concentration of urea or GdnHCl was determined by refractive index at 25 °C.[41] All other chemicals were reagent grade. Unlabelled and [6-^{19}F]Trp-labelled mADA were expressed in *Escherichia coli* strain W3110trpA33 using the construct pQE80L/mADA and purified as described.[14] Protein concentrations were determined using the Bio-Rad protein assay reagent.

Enzyme activity assays

ADA activity was measured on a Cary50Bio spectrophotometer (Varian) by following the rate of decrease of adenosine absorption at 265 nm at 20 °C. The enzyme specific activity was defined as one unit = 1 μmol of inosine produced min^{-1} mg^{-1}. The assay was initiated by addition of 5 μl of equilibrated enzyme sample to 995 μl of 75 μM adenosine in buffer with or without indicated denaturant. The concentration of enzyme in activity assay was 5 nM as determined by active-site titration with DCF.[20] Experiments were performed in 20 mM Tris–HCl (pH 7.4), 2 mM DTT, unless otherwise indicated.

CD and fluorescence spectroscopy

The far-UV CD spectra were measured on a Jasco-J715 spectropolarimeter with a 0.1 cm path-length cell using 10 μM protein at 20 °C. Spectra were recorded from 180–250 nm or from 200–250 nm. The fluorescence emission spectrum was measured on a PTI fluorometer (Photon Technology International, Inc.) using 1 μM protein at 20 °C.

Kinetic parameters of ADA as a function of urea concentration

The kinetic constants of mADA for adenosine were determined by simulation of progress curves. The kinetics experiments were carried out on an Applied Photophysics SX.18MV stopped-flow spectrofluorimeter (Leatherhead, UK) with 0.2 cm cell thermostatically controlled at 20 °C. ADA (final concentration of 0.1 μM) was equilibrated for two hours in urea before measurement. The progress curves of the ADA-dependent decrease of adenosine (final concentration of 10 μM and 50 μM) absorption were recorded. Kinetic constants from full time-course data were determined by fitting the set of progress curves to an appropriate mechanism using the program KINSIM.[17]

To address the urea-induced rapid change of the enzyme activity of mADA, kinetic constants at different concentrations of urea were measured as described above but using native enzyme instead of the protein sample pre-equilibrated in urea for two hours.

Inhibitor DCF binding and inhibition in the presence of varying urea

The rate constant of DCF (5 μM) binding to mADA (0.25 μM) in the presence of urea was measured using stopped-flow methods. The 1 μM DCF-induced-intrinsic fluorescence quenching of 0.5 μM mADA in the presence of urea was measured on the PTI fluorometer (Photon Technology International, Inc.). The inhibition of 0.05 μM mADA by 0.5 μM DCF was checked by following the time-course of the inhibition during the deamination of adenosine (50 μM) as catalyzed by the enzyme,[19] and the apparent k_{on} was determined by a computer simulation using the program KINSIM.[17]

^{19}F NMR spectroscopy

NMR spectra were recorded on a Varian Unity-Plus 500 MHz spectrometer operating at 470 MHz for ^{19}F nuclear spin using a Varian Cryo-Q dedicated 5 mm probe as described.[14] Data were acquired for 0.501 s using Varian VNMR s2pul pulse sequence and a spectral width of 6499.8 Hz. All spectra were collected with 1024 transients at 20 °C. The [6-^{19}F]Trp-labelled mADA (85 μM) was equilibrated in 0, 0.2, 0.5, 0.7, 1.0, and 3.0 M urea buffer at room temperature for 22 hours before collecting spectra. For the spectra of mADA bound with different inhibitors, 100 μM mADA and 200 μM inhibitor (DCF or PR) were used. The buffer used was 20 mM Tris–HCl (pH 7.4), 2 mM DTT, 5% (v/v) ^2H_2O and 0.1 mM [4-^{19}F]Phe (the internal reference of chemical shift).

Acknowledgements

We gratefully acknowledge Linda C. Kurz, Sydney D. Hoeltzli and James G. Bann for helpful discussion, and Robert Horton for technical assistance. This work is supported by NIH grant DK13332 to C. F.

References

1. Farber, G. K. & Petsko, G. A. (1990). The evolution of alpha/beta barrel enzymes. *Trends Biochem. Sci.* **15**, 228–234.
2. Brändén, C.-I. (1991). The TIM barrel–the most frequently occurring folding motif in proteins. *Curr. Opin. Struct. Biol.* **1**, 978–983.
3. Nagano, N., Orengo, C. A. & Thornton, J. M. (2002). One fold with many functions: the evolutionary relationships between TIM barrel families based on their sequences, structures and functions. *J. Mol. Biol.* **321**, 741–765.
4. Wierenga, R. K. (2001). The TIM-barrel fold: a versatile framework for efficient enzymes. *FEBS Letters*, **492**, 193–198.
5. Anantharaman, V., Aravind, L. & Koonin, E. V. (2003). Emergence of diverse biochemical activities in evolutionarily conserved structural scaffolds of proteins. *Curr. Opin. Chem. Biol.* **7**, 12–20.
6. Altamirano, M. M., Blackburn, J. M., Aguayo, C. & Fersht, A. R. (2000). Directed evolution of new catalytic activity using the α/β-barrel scaffold. *Nature*, **403**, 617–622.

7. Forsyth, W. R. & Matthews, C. R. (2002). Folding mechanism of indole-3-glycerol phosphate synthase from *Sulfolobus solfataricus*: a test of the conservation of folding mechanisms hypothesis in $(\beta\alpha)_8$ barrels. *J. Mol. Biol.* **320**, 1119–1133.
8. Höcker, B., Beismann-Driemeyer, S., Hettwer, S., Lustig, A. & Sterner, R. (2001). Dissection of a $(\beta\alpha)_8$-barrel enzyme into two folded halves. *Nature Struct. Biol.* **8**, 32–36.
9. Höcker, B., Jűrgens, C., Wilmanns, M. & Sterner, R. (2001). Stability, catalytic versatility and evolution of the $(\beta/\alpha)_8$-barrel fold. *Curr. Opin. Biotechnol.* **12**, 376–381.
10. Orengo, C. A., Jones, D. T. & Thornton, J. M. (1994). Protein superfamilies and domain superfolds. *Nature*, **372**, 631–634.
11. Wilson, D. K., Rudolph, F. B. & Quiocho, F. A. (1991). Atomic structure of adenosine deaminase complexed with a transition-state analog: understanding catalysis and immunodeficiency mutations. *Science*, **252**, 1278–1284.
12. Hershfield, M. S. & Mitchell, B. S. (2001). Immunodeficiency diseases caused by adenosine deaminase deficiency and purine nucleoside phosphorylase deficiency. In *The Metabolic and Molecular Bases of Inherited Disease* (Scriver, C. R., Beaudet, A. L., Sly, W. S. & Valle, D., eds), pp. 2585–2625, McGraw-Hill, New York.
13. Hershfield, M. S. (2003). Genotype is an important determinant of phenotype in adenosine deaminase deficiency. *Curr. Opin. Immunol.* **15**, 571–577.
14. Shu, Q. & Frieden, C. (2004). Urea-dependent unfolding of murine adenosine deaminase: sequential destabilization as measured by ^{19}F NMR. *Biochemistry*, **43**, 1432–1439.
15. Cooper, B. F., Sideraki, V., Wilson, D. K., Dominguez, D. Y., Clark, S. W., Quiocho, F. A. & Rudolph, F. B. (1997). The role of divalent cations in structure and function of murine adenosine deaminase. *Protein Sci.* **6**, 1031–1037.
16. Kurz, L. C., Weitkamp, E. & Frieden, C. (1987). Adenosine deaminase: viscosity studies and the mechanism of binding of substrate and of ground- and transition-state analogue inhibitors. *Biochemistry*, **26**, 3027–3032.
17. Barshop, B. A., Wrenn, R. F. & Frieden, C. (1983). Analysis of numerical methods for computer simulation of kinetic processes: development of KINSIM—a flexible, portable system. *Anal. Biochem.* **130**, 134–145.
18. Agarwal, R. P., Spector, T. & Parks, R. E., Jr (1977). Tight-binding inhibitors-IV. Inhibition of adenosine deaminases by various inhibitors. *Biochem. Pharmacol.* **26**, 359–367.
19. Frieden, C., Kurz, L. C. & Gilbert, H. R. (1980). Adenosine deaminase and adenylate deaminase: comparative kinetic studies with transition state and ground state analogue inhibitors. *Biochemistry*, **19**, 5303–5309.
20. Kurz, L. C., LaZard, D. & Frieden, C. (1985). Protein structural changes accompanying formation of enzymatic transition states: tryptophan environment in ground-state and transition-state analogue complexes of adenosine deaminase. *Biochemistry*, **24**, 1342–1346.
21. Danielson, M. A. & Falke, J. J. (1996). Use of ^{19}F NMR to probe protein structure and conformational changes. *Annu. Rev. Biophys. Biomol. Struct.* **25**, 163–195.
22. Wang, Z. & Quiocho, F. A. (1998). Complexes of adenosine deaminase with two potent inhibitors: X-ray structures in four independent molecules at pH of maximum activity. *Biochemistry*, **37**, 8314–8324.
23. Jiang, C. K., Hong, R., Horowitz, S. D., Kong, X. P. & Hirschhorn, R. (1997). An adenosine deaminase (ADA) allele contains two newly identified deleterious mutations (Y97C and L106V) that interact to abolish enzyme activity. *Hum. Mol. Genet.* **6**, 2271–2278.
24. Arredondo-Vega, F. X., Santisteban, I., Daniels, S., Toutain, S. & Hershfield, M. S. (1998). Adenosine deaminase deficiency: genotype-phenotype correlations based on expressed activity of 29 mutant alleles. *Am. J. Hum. Genet.* **63**, 1049–1059.
25. Ozsahin, H., Arredondo-Vega, F. X., Santisteban, I., Fuhrer, H., Tuchschmid, P., Jochum, W. *et al*. (1997). Adenosine deaminase deficiency in adults. *Blood*, **89**, 2849–2855.
26. Tsou, C. L. (1993). Conformational flexibility of enzyme active sites. *Science*, **262**, 380–381.
27. Tsou, C. L. (1995). Inactivation precedes overall molecular conformation changes during enzyme denaturation. *Biochim. Biophys. Acta*, **1253**, 151–162.
28. Tsou, C. L. (1998). Active site flexibility in enzyme catalysis. *Ann. N.Y. Acad. Sci.* **864**, 1–8.
29. Tsou, C. L. (1998). The role of active site flexibility in enzyme catalysis. *Biochemistry (Mosc.)*, **63**, 253–258.
30. Zhou, H. M., Zhang, X. H., Yin, Y. & Tsou, C. L. (1993). Conformational changes at the active site of creatine kinase at low concentrations of guanidinium chloride. *Biochem. J.* **291**, 103–107.
31. Xiao, G. S. & Zhou, J. M. (1996). Conformational changes at the active site of bovine pancreatic RNase A at low concentrations of guanidine hydrochloride probed by pyridoxal 5′-phosphate. *Biochim. Biophys. Acta*, **1294**, 1–7.
32. Liu, Z. J. & Zhou, J. M. (1995). Spin-labeling probe on conformational change at the active sites of creatine kinase during denaturation by guanidine hydrochloride. *Biochim. Biophys. Acta*, **1253**, 63–68.
33. Yang, H. J. & Tsou, C. L. (1995). Inactivation during denaturation of ribonuclease A by guanidinium chloride is accompanied by unfolding at the active site. *Biochem. J.* **305**, 379–384.
34. Kurz, L. C. & Frieden, C. (1987). Adenosine deaminase converts purine riboside into an analogue of a reactive intermediate: a ^{13}C NMR and kinetic study. *Biochemistry*, **26**, 8450–8457.
35. Thoma, R., Hennig, M., Sterner, R. & Kirschner, K. (2000). Structure and function of mutationally generated monomers of dimeric phosphoribosylanthranilate isomerase from *Thermotoga maritima*. *Structure*, **8**, 265–276.
36. Sánchez del Pino, M. M. & Fersht, A. R. (1997). Nonsequential unfolding of the β/α barrel protein indole-3-glycerol-phosphate synthase. *Biochemistry*, **36**, 5560–5565.
37. Eder, J. & Kirschner, K. (1992). Stable substructures of eightfold βα-barrel proteins: fragment complementation of phosphoribosylanthranilate isomerase. *Biochemistry*, **31**, 3617–3625.
38. Jasanoff, A., Davis, B. & Fersht, A. R. (1994). Detection of an intermediate in the folding of the $(\beta\alpha)_8$-barrel N-(5′-phosphoribosyl)anthranilate isomerase from *Escherichia coli*. *Biochemistry*, **33**, 6350–6355.
39. Bilsel, O., Zitzewitz, J. A., Bowers, K. E. & Matthews, C. R. (1999). Folding mechanism of the α-subunit of tryptophan synthase, an α/β barrel protein: global

analysis highlights the interconversion of multiple native, intermediate, and unfolded forms through parallel channels. *Biochemistry*, **38**, 1018–1029.
40. Silverman, J. A. & Harbury, P. B. (2002). The equilibrium unfolding pathway of a $(\beta/\alpha)_8$ barrel. *J. Mol. Biol.* **324**, 1031–1040.
41. Pace, C. N. (1986). Determination and analysis of urea and guanidine hydrochloride denaturation curves. *Methods Enzymol.* **131**, 266–280.
42. Koradi, R., Billeter, M. & Wüthrich, K. (1996). MOLMOL: a program for display and analysis of macromolecular structures. *J. Mol. Graph.* **14**, 51–55.

Edited by A. G. Palmer III

(Received 2 August 2004; received in revised form 13 October 2004; accepted 18 October 2004)